

## Supporting Information

# Wilkinson-type catalysts in ionic liquids for hydrogenation of small alkenes: understanding and improving catalyst stability

Eva Kratzer<sup>a†</sup>, Simon Schötz<sup>b†</sup>, Sven Maisel<sup>c</sup>, Dominik Blaumeiser<sup>b</sup>, Sharmin Khan Antara<sup>d</sup>, Leon Ewald<sup>d</sup>, Daniel Dotzel<sup>a</sup>, Marco Haumann<sup>d,e</sup>, Andreas Görling<sup>c</sup>, Wolfgang Korth<sup>a</sup>, Andreas Jess<sup>a,\*</sup>, Tanja Retzer<sup>b,\*</sup>

<sup>a</sup> Department of Chemical Engineering, University Bayreuth, Universitätsstraße 30, 95440 Bayreuth, Germany

<sup>b</sup> Interface Research and Catalysis, Erlangen Center for Interface Research and Catalysis, Friedrich-Alexander-Universität Erlangen-Nürnberg, Egerlandstraße 3, 91058 Erlangen, Germany

<sup>c</sup> Chair of Theoretical Chemistry, Friedrich-Alexander-Universität Erlangen-Nürnberg, Egerlandstraße 3, 91058 Erlangen, Germany

<sup>d</sup> Lehrstuhl für Chemische Reaktionstechnik (CRT), Friedrich-Alexander-Universität Erlangen-Nürnberg, Egerlandstraße 3, 91058 Erlangen, Germany

<sup>e</sup> Research Center for Synthesis and Catalysis, Department of Chemistry, University of Johannesburg, P.O. Box 524, Auckland Park 2006, South Africa

<sup>†</sup>shared first authorship

\*Corresponding author.

E-mail address: [jess@uni-bayreuth.de](mailto:jess@uni-bayreuth.de) (Andreas Jess).

E-mail address: [tanja.retzer@fau.de](mailto:tanja.retzer@fau.de) (Tanja Bauer).

## DRIFTS – Experimental procedure

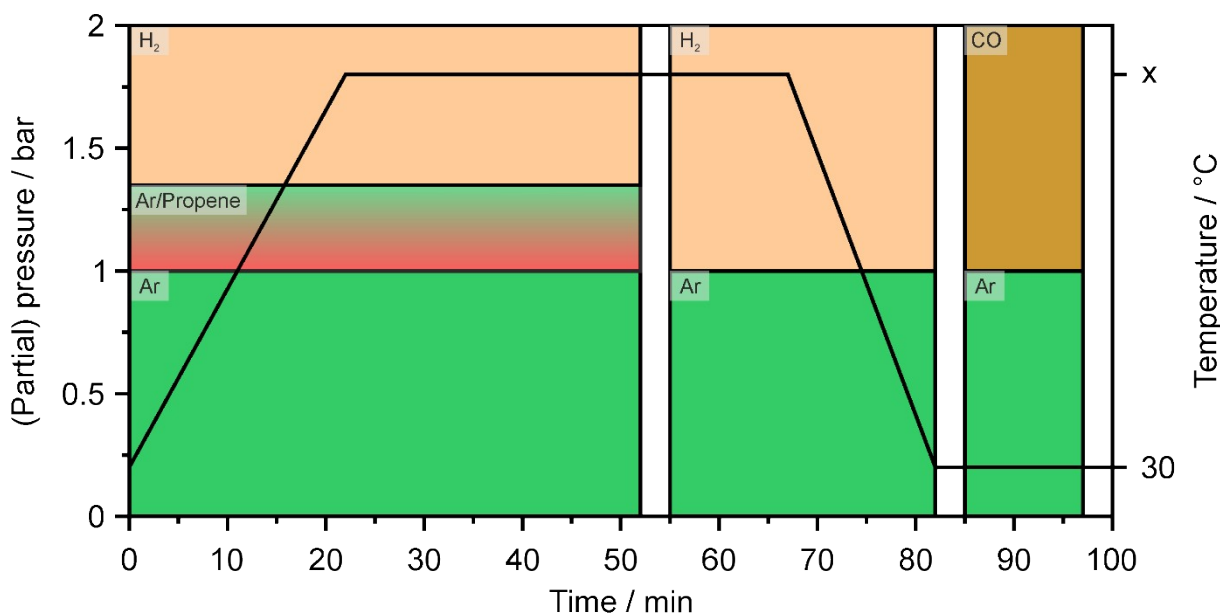


Figure S1: Experimental procedure for DRIFTS experiments.

## Hydrogenation with different 1-alkenes:

In preliminary hydrogenation experiments, the 1-alkene was varied. The used SILP catalyst (**Rh-1-SILP**) was synthesized as described in 2.1 (main manuscript) with pre-calcined silica (3.50 g, pore volume 0.647 cm<sup>3</sup>/g, Sigma Aldrich) as porous support, Trihexyltetradecylphosphonium chloride (0.7053 g, Cytec) as IL and 0.0623 g Wilkinson's catalyst (Acros Organics) were used. The experiments were carried out at  $T_{\text{reactor}} = 60\text{ °C}$ ,  $V_{\text{tot}} = 3.6\text{ l/h}$ ,  $p_{\text{tot}} = 2\text{ bar}$  with ratio of hydrogen to 1-Olefine of 2 : 1. Only the experiments for the hydrogenation of  $\alpha$ -butylene were performed at atmospheric pressure and thus the double amount of catalyst, 2 g instead of 1 g was used.

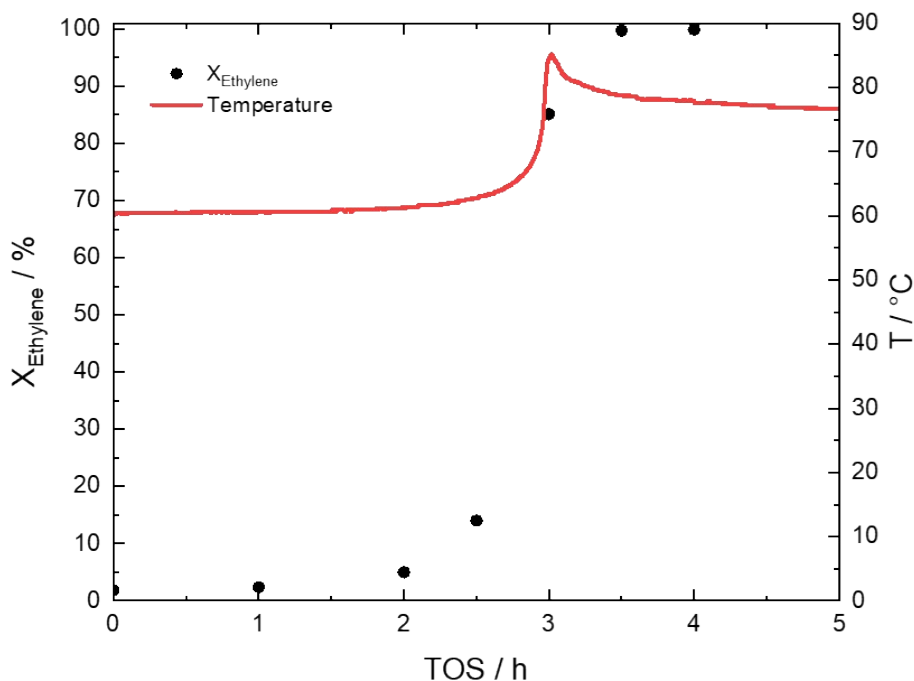


Figure S2: Hydrogenation of ethylene with  $m(\text{Rh-1-SILP}) = 1\text{ g}$ , the reactions conditions were  $T = 60\text{ °C}$ ,  $V_{\text{tot}} = 3.6\text{ l/h}$ ,  $p_{\text{tot}} = 2\text{ bar}$  with  $p_{\text{Ethylene}} = 0.67\text{ bar}$ , with a reactant ratio of 2 : 1 with H<sub>2</sub> : ethylene.

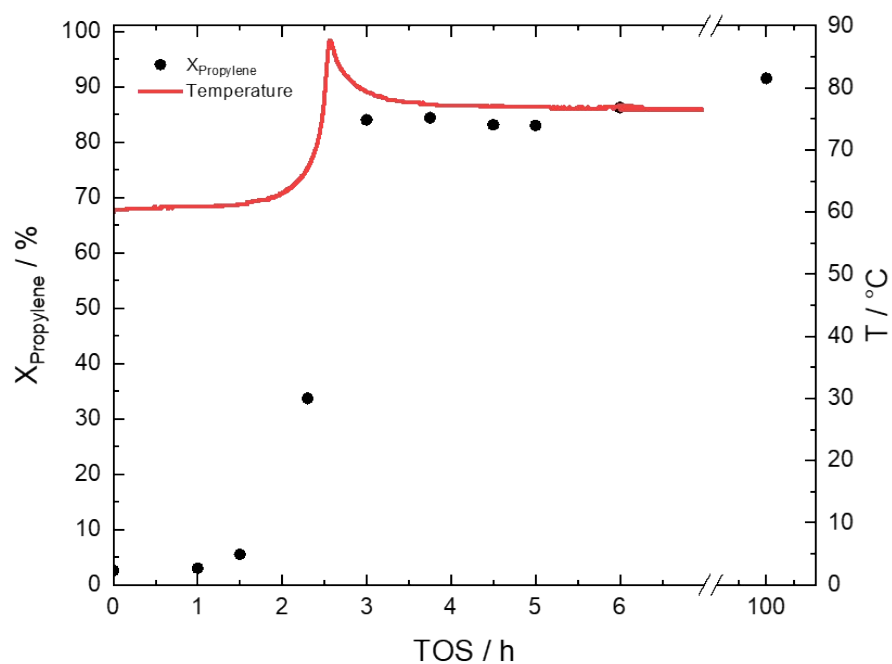


Figure S3: Hydrogenation of propylene with  $m(\text{Rh-1-SILP}) = 1\text{g}$ , the reactions conditions were  $T = 60\text{ }^\circ\text{C}$ ,  $V_{\text{tot}} = 3.6\text{ l/h}$ ,  $p_{\text{tot}} = 2\text{ bar}$  with  $p_{\text{Ethylene}} = 0.67\text{ bar}$ , with a reactant ratio of 2: 1 with  $\text{H}_2$  : ethylene.

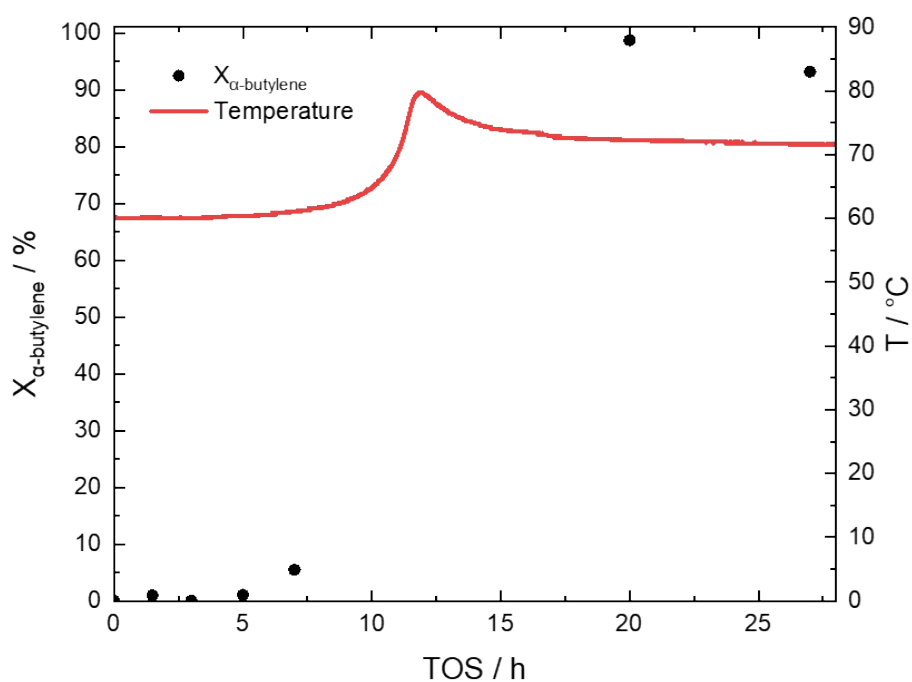


Figure S4: Hydrogenation of  $\alpha$ -butylene with  $m(\text{Rh-1-SILP}) = 2\text{ g}$ , the reactions conditions were  $T = 60\text{ }^\circ\text{C}$ ,  $V_{\text{tot}} = 3.6\text{ l/h}$ ,  $p_{\text{tot}} = 1\text{ bar}$  with  $p_{\text{Ethylene}} = 0.67\text{ bar}$ , with a reactant ratio of 2: 1 with  $\text{H}_2$  : ethylene.

## Hydrogenation of propene in a pool reactor

The pool reactor has been developed by the workshop of *Lehrstuhl für Chemische Reaktionstechnik* (CRT). By means of a pool reactor, a limiting case of SILP catalysts is considered. Here, a comparatively thick film of 500  $\mu\text{m}$  is used, which is approx. four order magnitude thicker than the films inside the SILP catalysts used. Interactions of the ionic liquid phase with the porous support surface are eliminated. Since there is no mixing with the gas phase or a second liquid phase, it can be assumed that the reaction occurs predominantly in the upper surface near region. Figure S5 depicts the assembled pool reactor as well as details on the inner design.

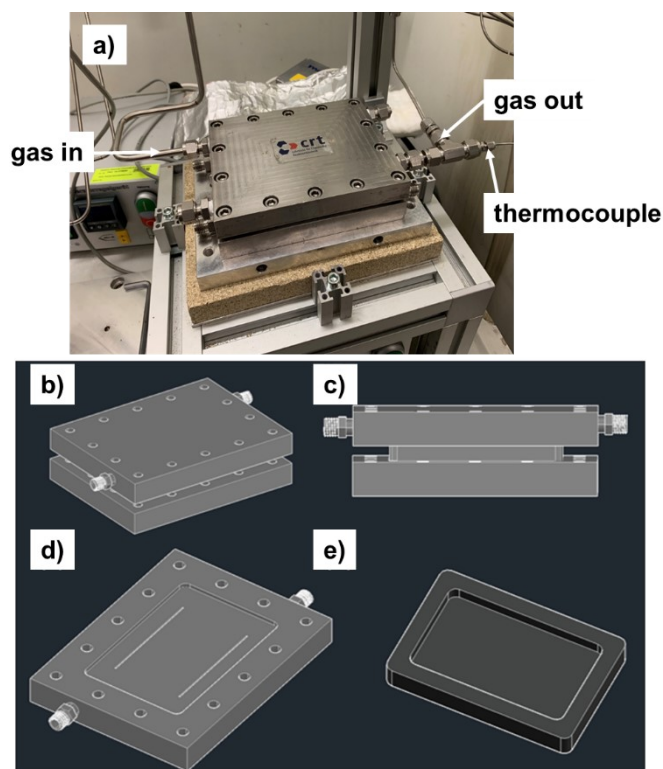


Figure S5: Photographs of a) assembled pool reactor with gas inlet and outlet; b) and c) CAD drawing of assembled reactor parts; d) upper lid and e) pool inlet.

To test the catalyst systems in the pool reactor, the required amount of ionic liquid was calculated to achieve a homogeneous film thickness of 500  $\mu\text{m}$ . The ionic liquid was weighed into a Schlenk flask under an inert argon atmosphere inside a glove box (Company: Vacuum Atmospheres Company, Model: OMNI-LAB) using a 5 ml syringe with a cannula. In a next step, the catalyst was also weighed inside the glove box. The flask was removed from the glovebox and connected to a Schlenk line. After careful evacuation and flushing with argon (three times), 5 to 10 ml of dichloromethane were added using a syringe, yielding a homogeneous yellowish solution. After adding the dichloromethane to the solution, the Schlenk flask was attached to a rotary evaporator. Under mild vacuum at 40  $^{\circ}\text{C}$ , the dichloromethane was withdrawn.

The pool reactor is opened and the upper closure part separated from the periphery and removed. The catalyst solution was transferred from the Schlenk flask using a gas-tight syringe and distributed as uniformly as possible in the pool compartment, while a low flow of helium ensured no contamination with air/moisture. The cover lid was placed on top and the four screws at the corners of the lid were tightened evenly to prevent the reactor trough from tilting. The periphery was connected and the helium flow was set to 10  $\text{mL}_\text{N} \text{ min}^{-1}$  while the reactor was heated to the desired

reaction temperature. Once the temperature equilibrated, the flow of helium was replaced by hydrogen and propene.

For analysis, an online gas chromatograph (Varian model 3900) was used, equipped with a PoraPLOT Q-HT column with a length of 30 m and a diameter of 0.32 mm (film thickness 10  $\mu\text{m}$ ) and a flame ionization detector. Areas were calibrated by known amounts of propene and propane.

Figure S6 shows the conversion of propene over 50 h time on stream in the presence of the Wilkinson complex dissolved in the ionic liquid  $[\text{C}_4\text{C}_1\text{Im}][\text{NTf}_2]$ .

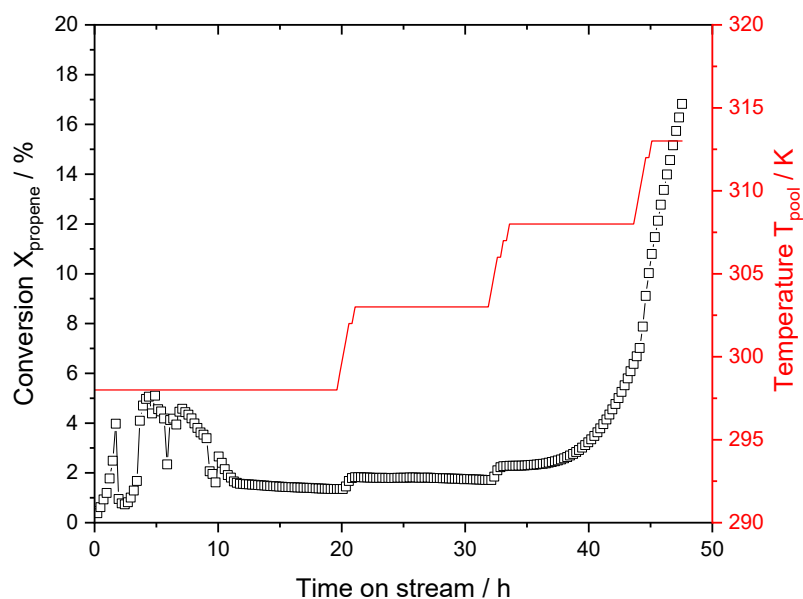


Figure S6: Hydrogenation of propene in the presence of  $\text{RhCl}(\text{tpp})_3$  dissolved in  $[\text{C}_4\text{C}_1\text{Im}][\text{NTf}_2]$ . Rh-complex = 8.3 mg, ionic liquid = 4.6 g,  $\text{H}_2 = 6.66 \text{ ml}_N \text{ min}^{-1}$ , propene =  $3.33 \text{ ml}_N \text{ min}^{-1}$ ,  $p = 6 \text{ bar(a)}$ ,  $T = 298 - 313 \text{ K}$ .

The catalyst solution turned from yellow into a dark one after the reaction, as depicted in Figure S7.

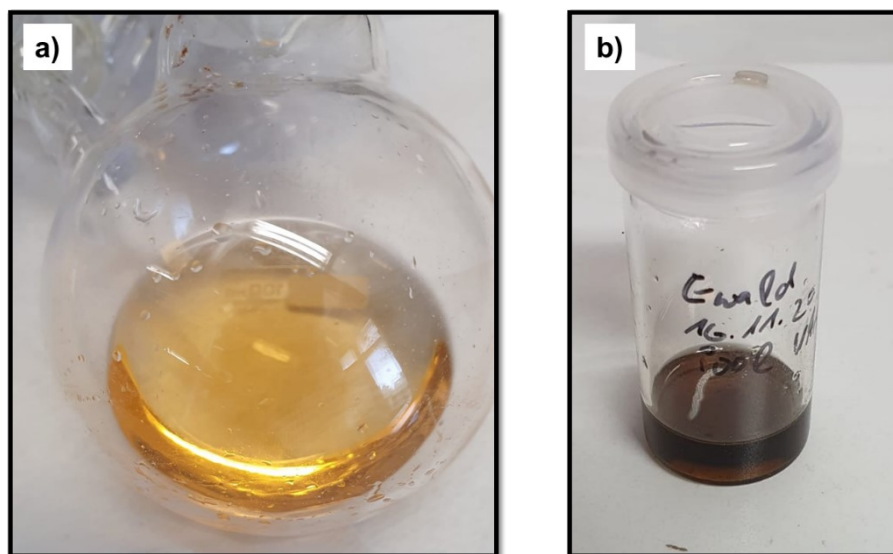


Figure S7: Photographs of a) fresh catalyst solution and b) spent solution after 50 h reaction.

### Reaction in toluene:

The hydrogenation of ethylene with Wilkinson's catalyst in toluene was performed in a semi-batch continuous stirred tank reactor. To that aim, the reactor was filled with 25 ml of the reaction solution ( $\beta_{\text{catalyst}} = 0.5 \text{ mg/mL}$ ), which was prepared under argon atmosphere. Afterwards the reactor was flushed with nitrogen to remove air before the reaction parameters were set to  $p_{\text{tot}} = 5 \text{ bar}$  ( $\text{H}_2 : \text{N}_2 : \text{ethylene} = 2 : 2 : 1$ )  $T_{\text{reactor}} = 60 \text{ }^\circ\text{C}$ ,  $V_{\text{tot,STP}} = 3.6 \text{ l/h}$  and stirring speed of 700 rpm. After 30 minutes run-in period a conversion of ethylene of 6.8% was achieved.

### Color Change in **Rh-1-SILP**:

For the hydrogenation reactions of 1-olefines a discoloration of the used SILP-catalyst was observed. In Figure S8, the discoloration of **Rh-1-SILP** (containing trihexyltetradecylphosphonium chloride and Wilkinson's catalyst, see below) can be seen, which was used in preliminary experiments.

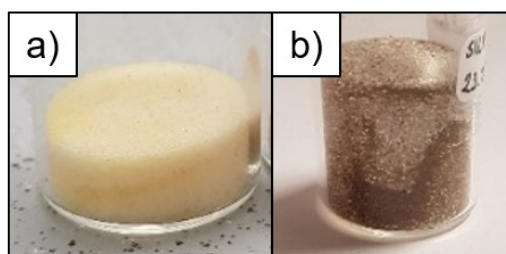


Figure S8: In a) the **Rh-1-SILP** before the hydrogenation reaction is shown with a pale-yellow color and in b) the discolored brown **Rh-1-SILP** is shown.

### UV/Vis spectroscopic determination of Cl<sup>-</sup>

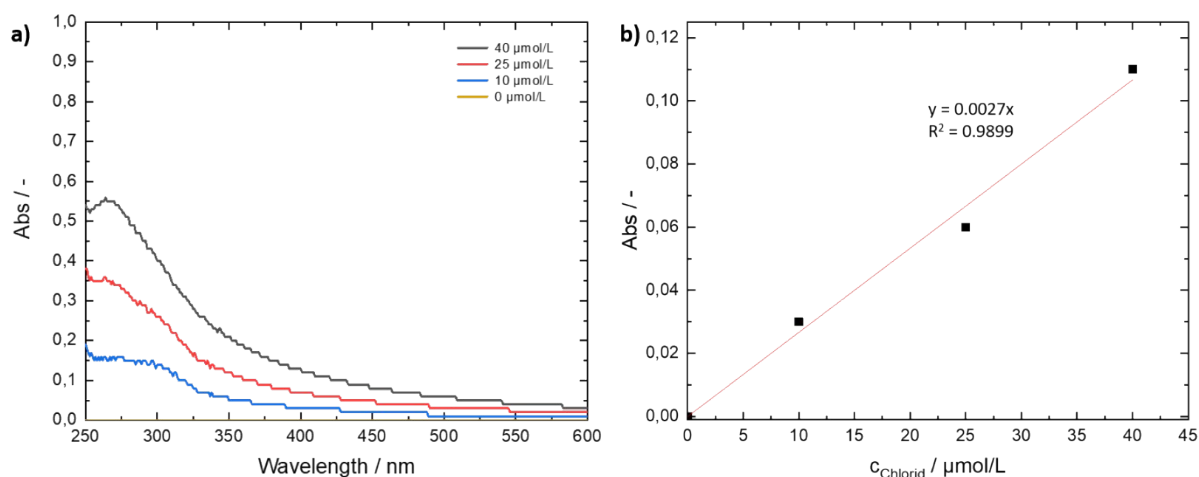


Figure S9: In a) the blanked UV/Vis-spectra of calibration solutions are shown, b) shows the resulting calibration curve with the absorbance at a wavelength of 420 nm.

In order to determine the  $\text{Cl}^-$  concentration, we pass the product gas stream of the hydrogenation reaction through an aqueous  $\text{AgNO}_3$  solution acidified with nitric acid. Due to safety reasons (glass washing bottle) the total pressure was reduced to 2 bar in this experiment, while the other reaction parameters were kept at the default reaction conditions. In the course of the reaction, the clear solution turned into a cloudy liquid due to precipitated  $\text{AgCl}$ . After 24 h TOS, 71% of the chloride ions had been removed from the SILP catalyst as determined by means of UV/Vis-spectroscopy. The white

precipitate (AgCl) dissolved upon addition of a few drops of ammonia and darkened upon exposure to daylight due to disintegration into  $\text{Cl}_2$  and Ag. Both test experiments prove that the precipitate is indeed AgCl and, thus, Cl-elimination from Wilkinson's catalyst occurred. We further exclude that the received white cloudy precipitate is related to the presence of the  $\text{NTf}_2^-$  anion in the used IL, as dissolution of  $\text{LiNTf}_2$  in an aqueous  $\text{AgNO}_3$  solution acidified with nitric acid did not lead to precipitation.

The concentration of the precipitated chloride was determined via UV/Vis-spectroscopy (analytikjena, SPECORD/200 Plus). Therefore, a 0.1 M  $\text{AgNO}_3$ -solutions (acidified with  $\text{HNO}_3$ ) with different amounts of chloride ions were prepared and scanned in the UV/Vis spectrometer over a wavelength range of 290-600 nm (Figure S9 a). The calibration line (Figure S9b) was created at the absorbance values of the wavelength of 420 nm and changing the resulting linear equation to the following formula:

$$c_{\text{chloride, sample}} = x = \frac{y}{0.027}$$

the chloride concentration in the washing bottle of the examined sample could be defined with a value of 22  $\mu\text{mol/L}$ . The maximum chloride concentration of the SILP catalyst used here is 32  $\mu\text{mol/L}$ , so  $\sim 71\%$  was precipitated in the  $\text{AgNO}_3$ -solution. The SILP sample used for the chloride ion determination had the same components as the Rh-1-SILP sample, but with slightly different weights, which are given in Table S1.

Table S1: Composition of the examined SILP catalyst for the chloride-ion determination experiment.

compound	m [g]
Silica 150	1.5
$[\text{C}_4\text{C}_1\text{Im}][\text{NTf}_2]$	0.475
$[\text{RhCl}(\text{PPh}_3)_3]$	0.026

Enlarged DRIFT spectra for **Rh-1-SILP** and **Rh-SCILL**

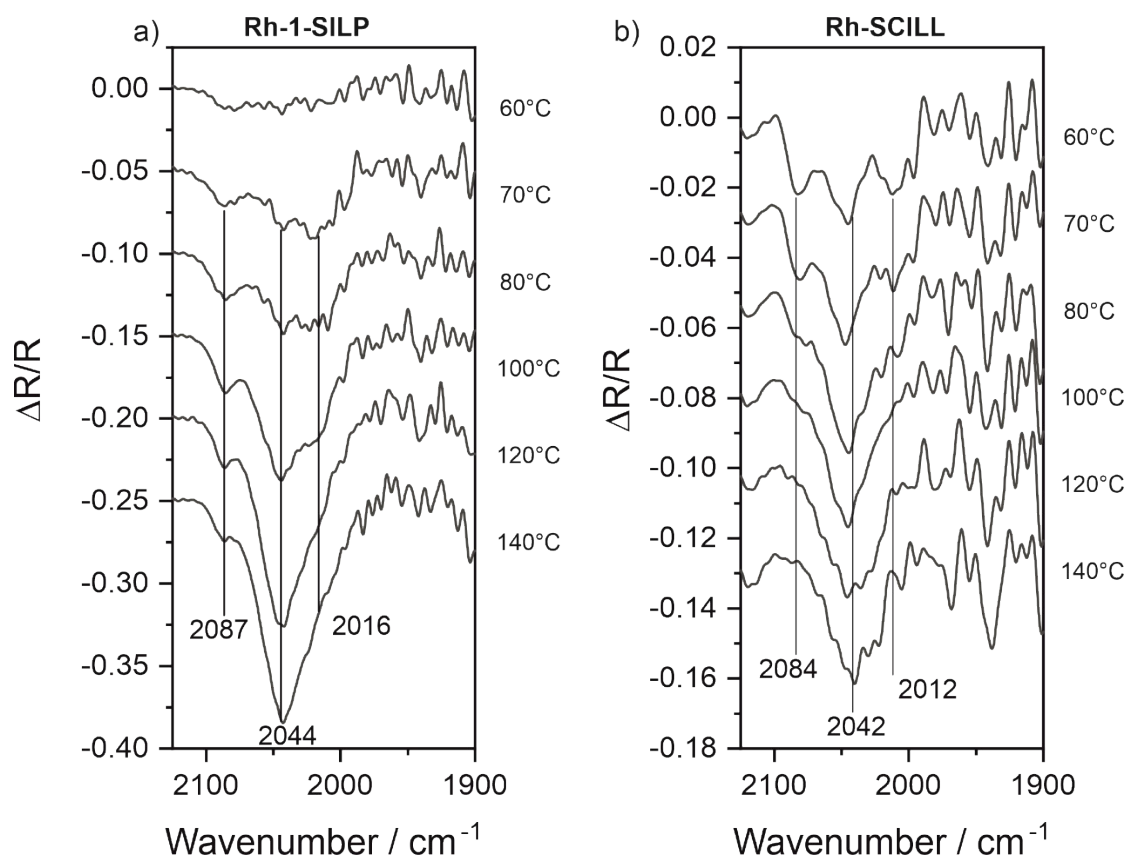


Figure S10: In situ DRIFT spectra acquired in 1 bar CO of a) Rh-1-SILP and b) Rh-SCILL, all heated in  $\text{H}_2/\text{Ar}$  atmosphere. For all DRIFT spectra the CO gas phase was subtracted mathematically.



### $^{31}\text{P}$ -NMR solid-state NMR spectra

In the three  $^{31}\text{P}$ -MAS-NMR spectra is further shown the used component with the respective structure formula. In Figure S11 the signal at -5.3 ppm is from the  $\text{PPh}_3$  the other peak small peak at  $\delta = 33.5$  ppm is assigned to an oxidized  $\text{PPh}_3$  species, and the  $^{31}\text{P}$ -MAS NMR spectra was recorded at 12.5kHz.

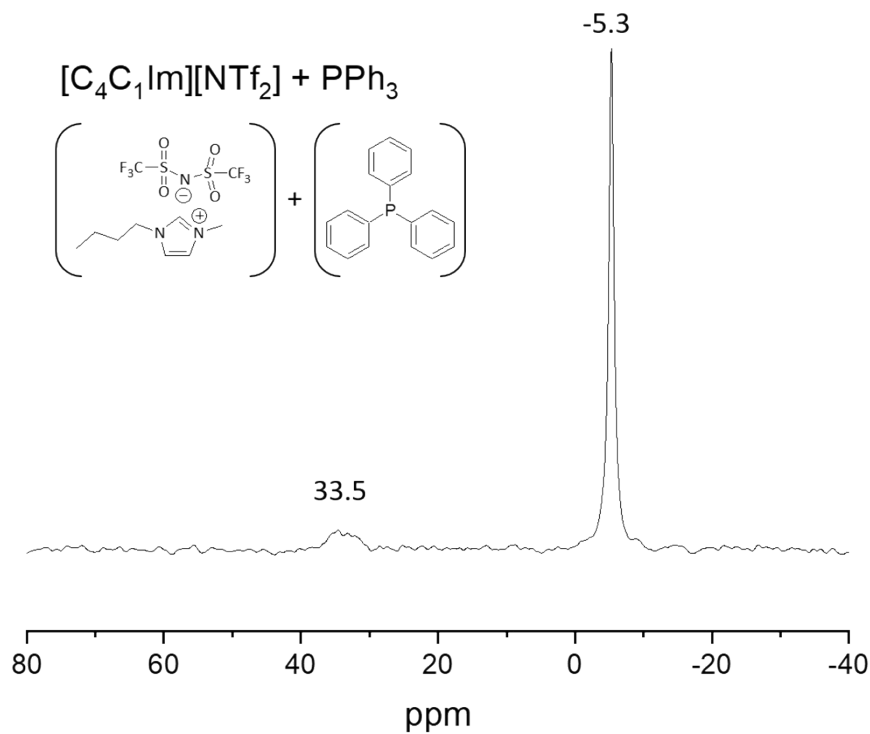


Figure S11:  $^{31}\text{P}$ -MAS-NMR spectra of Triphenylphosphine ( $\text{PPh}_3$ ) dissolved in  $[\text{C}_1\text{C}_4\text{Im}][\text{NTf}_2]$  recorded at 121.5 MHz and a spinning speed of 12.5 kHz.

Figure S12 shows the spectra of the dissolved Wilkinson's Catalyst in  $[\text{C}_1\text{C}_4\text{Im}][\text{NTf}_2]$  it was recorded at 5.0 kHz.

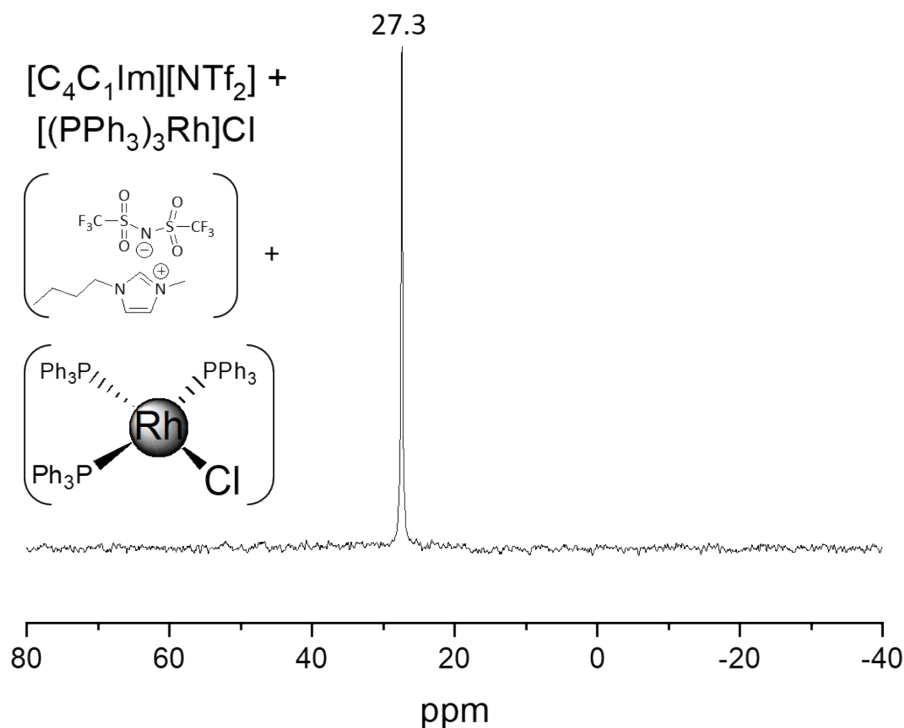


Figure S12:  $^{31}P$ -MAS-NMR spectra Wilkinson's catalyst dissolved in  $[C_1C_4Im][NTf_2]$  recorded at 121.5 MHz and a spinning speed of 5.0 kHz.

The  $^{31}P$ -MAS-NMR spectra of the neat Wilkinson's Catalyst was recorded at 12.5 kHz (Figure S13).

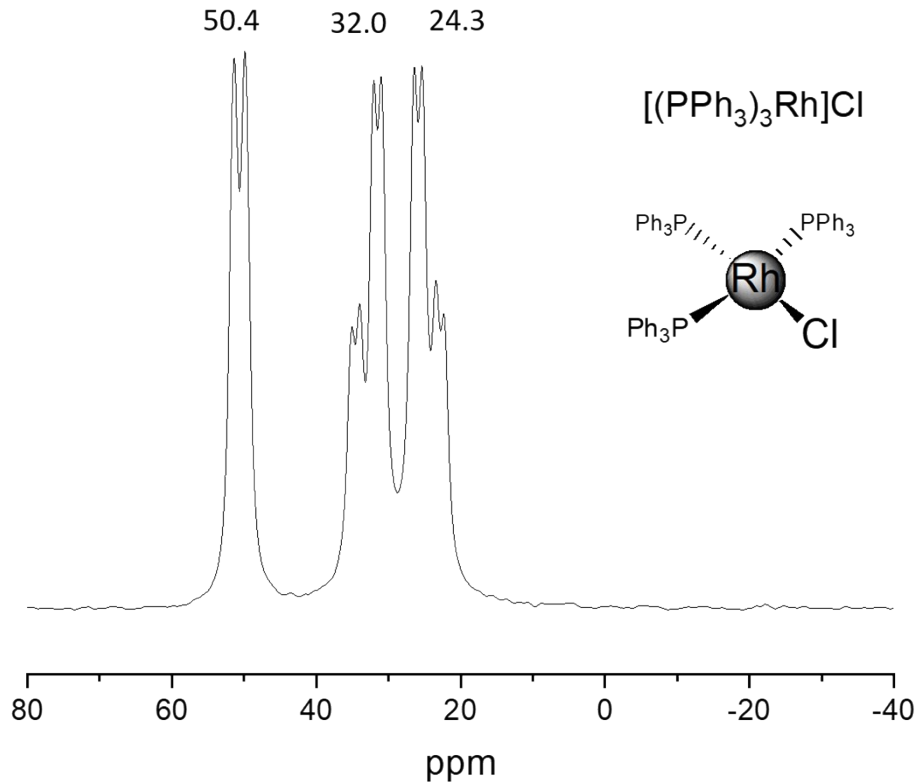


Figure S13:  $^{31}P$ -MAS-NMR spectra of the neat Wilkinson's Catalyst recorded at 121.5 MHz and a spinning speed of 12.5 kHz.  $^{31}P$ -NMR (121.5MHz):  $\delta$  (ppm) = 24.3 (dd,  $J(Rh-P) = 134$  Hz,  $J(P-P) = 378$  Hz,  $PPh_3$  cis to chloride), 32.0 (dd,  $J(Rh-P) = 134$  Hz,  $J(P-P) = 366$  Hz,  $PPh_3$  cis to chloride), 50.4 (d,  $J(Rh-P) = 183$  Hz,  $PPh_3$  trans to chloride).

### Variation of experimental conditions: CO in reactant stream

The first, crucial step towards NP formation is the consecutive loss of the ligands under hydrogenation reaction conditions. In contrast to the findings presented above, the used Rh-based catalyst is stable during SILP-catalyzed hydroformylation reactions, although reducing conditions in form of H<sub>2</sub> are present in both cases. One factor that could be responsible for the stabilization of the complex is the presence of CO in the reactant gas stream. Thus, we co-fed CO to the reactant gas stream of H<sub>2</sub> and ethylene in a series of experiments referred to as milder-hydroformylation conditions. To that aim, N<sub>2</sub> was partly substituted by CO. Figure 6 depicts the obtained experimental data and a comparison to the hydrogenation experiment. The results clearly show that hydrogenation of ethylene is almost zero and also NP formation does not occur at least for 24 h TOS in the presence of CO. This finding shows that a low CO partial pressure ( $p_{CO} = 0.07$  bar) is sufficient to prevent NP formation and, thus, hydrogenation caused by the NPs. It is important to note that no hydroformylation products were found in the product gas stream under the applied reaction conditions. However, we find small amounts of 1-propanal and ethane when setting the reaction conditions closer to hydroformylation conditions (see experimental section), i.e. higher total pressure and temperature. Please note that the stabilization via CO is temporary. Upon exchange of the CO reactant gas stream with N<sub>2</sub> after 24 h TOS, the same sigmoidal behavior as earlier mentioned can be seen. Thus, we assume that apart from overall harsher reaction conditions, the presence of CO stabilizes Wilkinson's catalyst during hydroformylation in SILP catalysts. Our results demonstrate that it is possible to exploit the stabilizing effect of gaseous CO during hydrogenation of small alkenes, however, the effect is intrinsically limited due to the competing hydroformylation reaction. Therefore, we test the incorporation of CO directly into the Rh-complex.

### Visualization of optimized complex structures:

*Table S2: Visualization of optimized complex structures in Table 4. Color scheme hydrogen (grey), carbon (black), nitrogen (blue), oxygen (red), phosphorus (dark green), sulfur (yellow), chlorine (light green), rhodium (pink).*

Species	Structure
<b>Monocarbonyl complexes</b>	
$[\text{RhCl}(\text{CO})(\text{PPh}_3)_3]$	
$[\text{Rh}(\text{CO})\text{H}(\text{PPh}_3)_3]$	
<i>cis</i> - $[\text{Rh}(\text{CO})(\text{NTf}_2)(\text{PPh}_3)_2]$ (1)	1
<i>trans</i> - $[\text{Rh}(\text{CO})(\text{NTf}_2)(\text{PPh}_3)_2]$ (2)	

--	--

	Dicarbonyl complexes
$trans\text{-}[\text{Rh}(\text{CO})_2(\text{PPh}_3)_2]$ (1)	
$cis\text{-}[\text{Rh}(\text{CO})_2(\text{PPh}_3)_2]$ (2)	
$[\text{RhH}(\text{CO})_2(\text{PPh}_3)_2]$ (1)	
$[\text{RhH}(\text{CO})_2(\text{PPh}_3)_2]$ (2)	

--	--

$[\text{RhH}(\text{CO})_2(\text{PPh}_3)(\text{NTf}_2)]$	
<b>Tricarbonyl complexes</b>	
$\textit{fac}\text{-}[\text{Rh}(\text{CO})_3\text{H}(\text{PPh}_3)] (1)$	
$\textit{mer}\text{-}[\text{Rh}(\text{CO})_3\text{H}(\text{PPh}_3)] (2)$	
<b>Complexes with bidentate ligands</b>	
$[\text{Rh}(\text{acac})(\text{CO})(\text{NTf}_2)]$	



[Rh(CO)(NTf <sub>2</sub> )(xantphos)] (1)	
[Rh(CO)(NTf <sub>2</sub> )(xantphos)] (2)	

In situ Rh-4-SILP DRIFTS experiment:

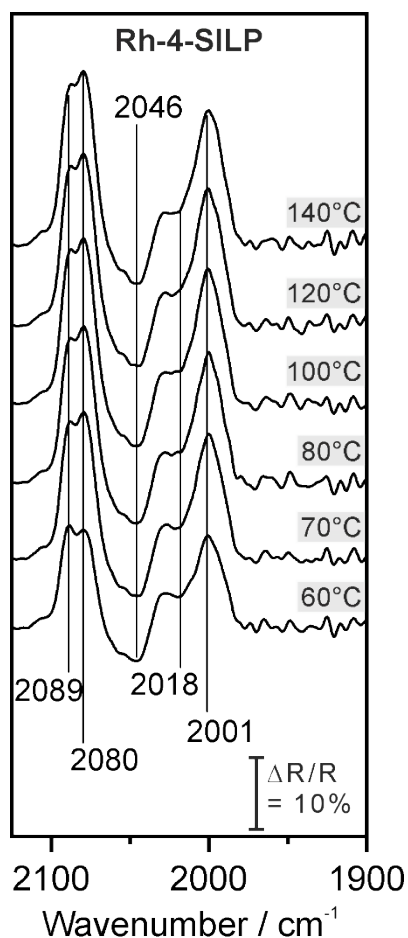


Figure S14: In situ DRIFT spectra acquired in 1 bar CO, **Rh-4-SILP** heated in H<sub>2</sub>/Ar atmosphere. CO gas phase was subtracted mathematically.

After heating **Rh-4-SILP** to 60°C, we observe three upwards pointing peaks at 2089, 2080, and 2001 cm<sup>-1</sup>, a shoulder at 2018 cm<sup>-1</sup>, and a downwards pointing peak at 2046 cm<sup>-1</sup>. During the whole experiment, there is no change in the peak position and no additional peaks are formed.

The band at 2046 cm<sup>-1</sup> indicates CO<sub>on-top</sub> on Rh<sup>0</sup>-NP already after heating the sample to 60°C.

Color Change in **Rh-4-SILP** and **xt-Rh-4-SILP**:

In Figure S15 a) the **xt-Rh-4-SILP** with Xantphos of a pale-yellow color can be seen on the left before and on the right after hydrogenation. In b) the **Rh-4-SILP** (without Xantphos) is shown, on the left it can be seen with its pale-yellow color before the hydrogenation and on the right the SILP has turned brownish-black after the hydrogenation.

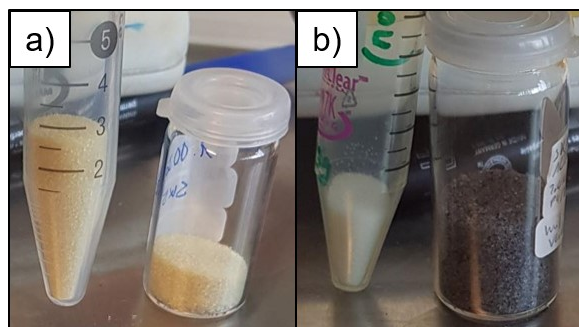


Figure S15: In a) the **xt-Rh-4-SILP** before (left) and after (right) hydrogenation with ethylene are shown, both have a pale-yellow color. In b) the **Rh-4-SILP** are shown left is for hydrogenation with a pale-yellow color and after hydrogenation the color changed to brownish-black (right).